# Epitaxial ZnO Nanowire-on-Nanoplate Structures as Efficient and Transferable Field Emitters

*Jizhong Song, Sergei A. Kulinich, Jian Yan, Zhigang Li, Jianping He, Caixia Kan, and Haibo Zeng**

As materials with a tremendously wide variety of potential applications, ZnO nanostructures have attracted a lot of attention in recent years.[1–9] Among them, vertical one-dimensional (1D) ZnO nanostructures such as nanowires, nanorods, and nanotips have been considered as excellent candidates for electron field emitters as they have low work functions, high aspect ratios, high mechanical stability, and high conductivity.[10–15] The field emission (FE) performance of such materials is highly affected by their intrinsic physical and structural parameters, such as alignment, density, uniformity, and tapering. After being stimulated by an applied electric field and before reaching the counter electrode, electrons have to pass through the interface between the 1D ZnO structure and substrate. However, irrespective of the synthetic route used (whether chemical or physical), all known vertical ZnO emitters prepared on heterogeneous substrates demonstrate a so-called 'dead' layer, which is associated with a low crystallinity and poorly ordered region at the emitter–substrate interface.[16,17] To date, this is one of the major and universal obstacles hindering the wide use of 1D ZnO in electronic and optoelectronic devices, such as solar cells,[18] photodetectors,[19] light-emitting diodes,[20] and field emitters.[21] Obviously, growing 1D ZnO epitaxially on ZnO subtrates would provide a sharp and high-quality interface, which is favorable for FE performance. However, no single-crystal ZnO wafers with low cost are available for the moment, and the related technology also needs to be improved. Therefore, achieving the high-quality interface with the substrate is still a major challenge for the electronic and optoelectronic applications based on 1D ZnO nanomaterials.

J. Z. Song, Prof. H. B. Zeng
Optoelectronic Nanomaterials Center
College of Materials Science and Engineering
Nanjing University of Science and Technology
Nanjing 210094, PR China
E-mail: zeng.haibo.nano@gmail.com
J. Z. Song, Prof. J. P. He, Prof. C. X. Kan,
Prof. H. B. Zeng
State Key Laboratory of Mechanics and Control of Mechanical Structures, College of Materials Science and Technology
Nanjing University of Aeronautics and Astronautics
Nanjing 210016, PR China
Prof. S. A. Kulinich
Institute of Innovative Science and Technology
Tokai University, Hiratsuka
Kanagawa 259–1292, Japan
Dr. J. Yan and Z. G. Li
Key Laboratory of Materials Physics, Institute of Solid State Physics
Chinese Academy of Sciences
Hefei 230031, PR China

DOI: 10.1002/adma.201302293

Here, we demonstrate a new strategy that utilizes hexagonal ZnO nanoplates as homogeneous nanoscale substrates for the epitaxial growth of ZnO nanowires, which results in very sharp and highly ordered interfaces and thus improves the product FE performance. Interestingly, a highly selective growth of only one nanowire at the center of each nanoplate has been acheived with a high yield and reproducibility. Furthermore, owing to the free-standing nature of such wire-on-plate (WOP) nanostructures, as well as their capability to self-assemble vertically, the product is demonstrated to be easily exfoliated and transferred onto other substrates, including flexible ones, thus showing great potential for the fields of flexible electronics and photonics.

Pre-synthesized ZnO hexagonal nanoplates with diameters of 200–400 nm and thicknesses of ≈20 nm were spin-coated on Si wafers (Figure S1, Supporting Information) and were then used as substrates for a subsequent chemical vapor deposition (CVD) stage. Electronic microscopy images of resulted ZnO nanostructures are presented in **Figure 1**. As shown in Figure 1a, the yield is very large, and the product is very pure and uniform, exhibiting no byproducts that are common for conventional CVD, such as nanobelts and nanohelixes.[22,23] The wire length was time-dependent and could reach more than 10 μm after 60 minutes of growth. Figure 1b reveals that the diameter of the wires is ≈50 nm and is uniform through the entire wire length. Very interestingly, it can clearly be seen in Figures 1b,c that each nanowire was grown at the very center of the ZnO nanoplate substrates. It was very hard to find nanoplates hosting two or more wires. This implies that the proposed approach provides a highly selective growth of ZnO single WOPs, which has not been reported so far to the best of our knowledge.

The interface between the ZnO wires and nanoplate substrates is seen in Figure 1c and in Figure S2, Supporting Information, to be very sharp. We did not find any signs of a poorly ordered and/or polycrystalline interlayer, which usually appears in ZnO nanowires CVD-grown on Si and sapphire substrates and ZnO arrays chemically grown on glass substrates.[24,25] On the contrary, as a result of epitaxial growth, the whole WOP structures were observed to be single-crystalline. The hexagonal ZnO nanoplates used as a nanoscale substrate in this work are well-known to have the [0001] direction normal to their surface, which is just the growth direction of 1D ZnO nanowires (see Figure S3, Supporting Information). The grown ZnO nanowires were confirmed by high-resolution transmission electron microscopy (HRTEM) to have the same orientation. Figure 1d shows a very neat and smooth surface of a nanowire segment with a single-crystalline structure. The HRTEM image in Figure 1e exhibits lattice fringes of 0.52 nm, corresponding

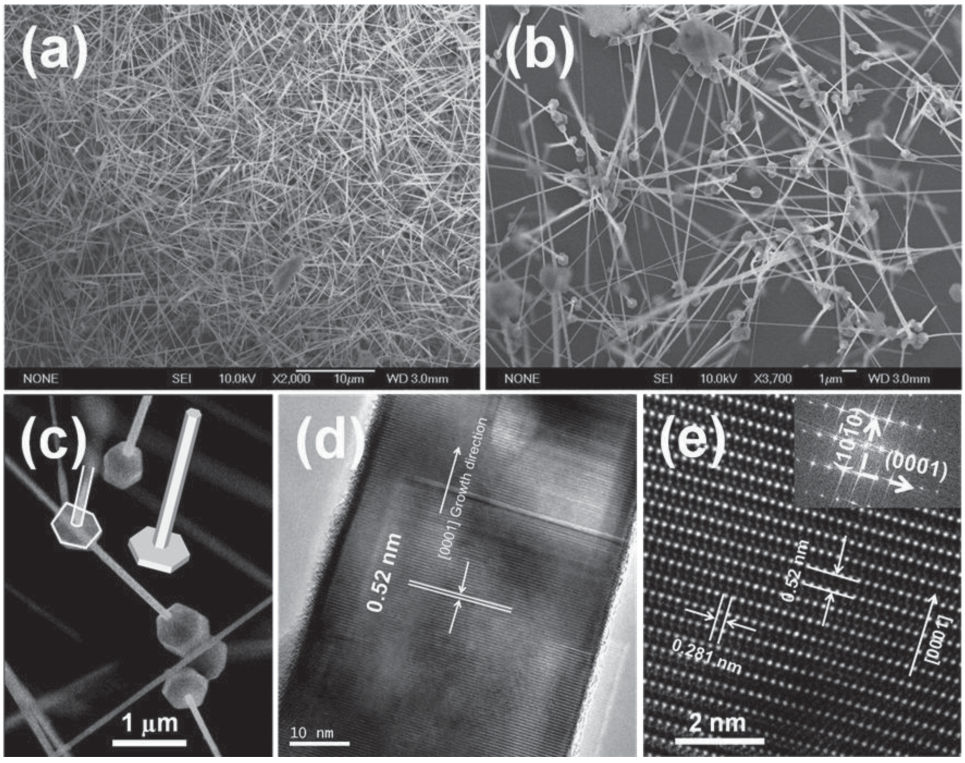


**Figure 1.** a,b) Field-emission scanning electron microscope (SEM) images of as-grown ZnO WOP structures with growth time of 60 min taken at different magnifications. c) High-magnification SEM image of as-grown ZnO WOP structures grown for 60 min, showing an outline of nanoplate and nanowire drawn in gray color and a schematic presentation given, as inset. d) High-resolution transmission electron microscopy (HRTEM) image of a ZnO nanowire. e) Magnified HRTEM image of the ZnO nanowire in panel d and its fast Fourier transform (FFT) pattern (inset).

to the (0001) plane normal to the growth direction, which is consistent with that of wurtzite ZnO. The HRTEM image in Figure 1e does not reveal any visible defects and reflects a perfect lattice. The FFT pattern shown as inset in Figure 1e also confirms the ZnO nanowires have a good crystallinity, exhibiting a set of reflections corresponding to the [0001] crystallographic direction of ZnO and being consistent with Figure 1d. The results presented in Figure 1 prove that the nanowires are indeed *c*-axis-oriented, corresponding to the vertical direction of the used nanoplate substrates and implying the epitaxial relationship within the entire WOP structures. Importantly, such highly crystalline nail-like structures are very likely to decrease the electron loss at the interface, thus favoring electron transport and improving FE performance.

While the nanowires were found to be selectively grown at the nanoplate centers, the ZnO plates themselves had very poor adhesion to the Si substrate. This is clearly seen in Figures 1a,b, where most nanoplates are lifted off the substrate as a result of the interplay and interaction between their nanowires. This implies that the novel WOP nanostructures can be easily exfoliated and transferred onto a new substrate. As shown in **Figure 2**a, on sonication, the material formed a dispersion in ethanol. By dropping the dispersion onto another substrate, we could transfer the WOP structures onto a new substrate (including a flexible PET), as shown in Figure 2b.

The gray area observed in Figure 2b where the WOP material was transferred remained unchanged after bending several times. Note that conventional CVD-prepared 1D ZnO nanostructures are not proper for flexible electronics and photonics because the corresponding substrates cannot survive the high temperatures necessary for the growth of such nanomaterials.[26,27] Therefore, the materials reported in this study, being transferable, open a new avenue for the development of flexible field emitters. It is also important to mention that, during ethanol evaporation, the WOP structures could self-align vertically on a new substrate, which is also very attractive from a practical point of view. The side-view SEM image in Figure 2c exhibits that most of the ZnO WOP structures are vertically oriented on their new substrate, and only a small fraction lie horizontally. This finding could be explained by the steric effect of the nanowires, which could make them align and orient vertically as the dispersion evaporates. At the same time, the flat ZnO nanoplates are also prone to align parallel to the substrate surface, thus also orienting the WOP structures vertically, in contrast to the previously reported ZnO nanowires grown on Si.[2,28] The observed verticality and high density of the ZnO nanowires are expected to reduce the screening effect during electron field emission, as additionally supported by the top-view image in Figure 2d.[11,12]

Since the growth of various ZnO materials along the *c*-axis is well known in the literature,[23,29–32] the key factor for the formation of the present WOP structures is their highly selective nucleation at the center of nanoplates. This can be explained by the high activity of the center sites of the used nanoscale substrates. Although there are not yet any reports of such a highly preferential nucleation and growth at the center of the (0001)

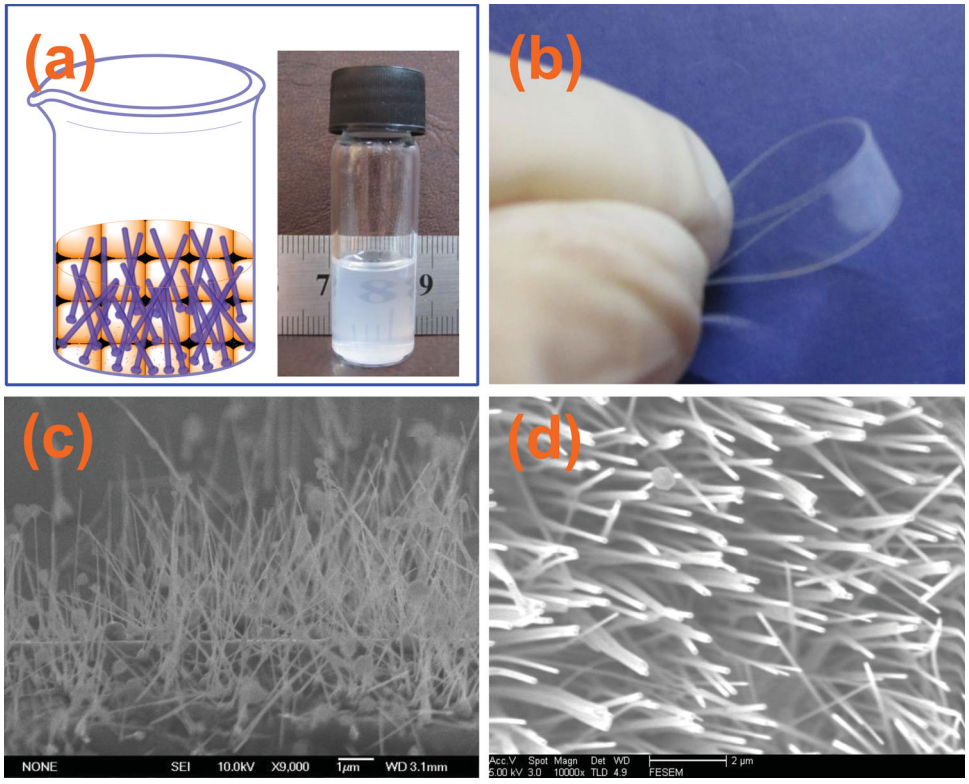


**Figure 2.** a) Ethanol dispersion of ZnO WOP structures (shown schematically, left) and a real sample (right). b) Sample of ZnO WOP structures transferred onto flexible polyethylene terephthalate (PET)/indium tin oxide (ITO) substrate. c) Tilted-view, and d) top-view SEM images of ZnO WOP structures transferred on a new Si substrate.

ZnO facet, its high activity, which is normally associated with a high surface energy, has been revealed in 'selective etching' experiments reported by several groups.[33–35] For instance, the central area of the (0001) plane was observed to be preferentially etched first when ZnO nanotubes were prepared on hexagonal ZnO prisms.[35]

As is well known, surface defects with high surface free energy act as nucleation sites to induce selective growth along a preferential growth direction.[36,37] Therefore, we believe that it is the high defect density at ZnO nanoplate centers, along with the high mobility of deposited ZnO species, that was responsible for the formation and growth of the WOP structures reported in this work (see **Figure 3**). To verify this hypothesis, we tested the effect of synthesis temperature on the product morphology. At lower temperatures (850 °C), the products grown on ZnO nanoplates were film-like structures (Figure S4a, Supporting Information), which is clearly related to a reduced mobility of deposited ZnO species. As the CVD temperature was elevated to 1050 °C, nanowire arrays were observed to form and to grow on each ZnO nanoplate (see Figure S4b, Supporting Information). This is explained by a very high surface mobility of deposited species and easier redistribution of surface defects, which probably resulted from surface restructuring. The unique ZnO WOP structures were obtained only at temperatures of approximately 950 °C (that is, within the range where the deposited species were mobile enough to nucleate only at the highest-energy defect sites) while the latter surface defects could not be reconstructed and redistributed on the nanoplate surface.

On the basis of the above, we comment a possible mechanism of the ZnO WOP formation as follows. At a proper process

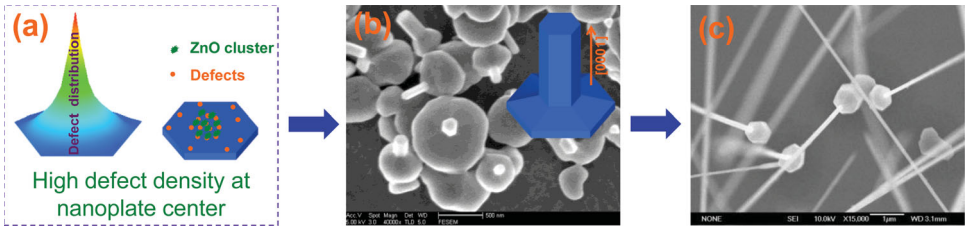


**Figure 3.** Illustration of the epitaxial growth of a single ZnO nanowire on a ZnO nanoplate. a) Schematic defect density distribution on the ZnO nanoplate surface and ZnO cluster formation at the nanoplate center. b) ZnO cluster nucleation becoming ZnO sprouts with a sketch of the [0001] growth direction as inset. c) Further nanowire growth along the [0001] direction and formation of ZnO WOP structures after a growth time of 60 min.

temperature, the high-defect-density zones (located primarily at the nanoplate centers) facilitate nucleation of incoming ZnO species at these sites, as shown in Figure 3a. Subsequently, the formed ZnO nuclei quickly induce a selective growth along its preferential growth direction, as schematically illustrated in the inset of Figure 3b. The as-formed ZnO 'sprouts' were clearly observed after 5 min of growth (Figure 3b). As time elapses, the ZnO formations grow longer and become nanowires (see, for example, Figure S5c, Supporting Information, for a sample grown for 20 min). Eventually, ZnO WOP structures with wires as long as 10 μm were obtained after 60 min, as seen in Figure 3c. More detailed comparison of the ZnO WOP structures prepared after different growth times is given in Figure S5, Supporting Information. As the wires grow longer, the ZnO substrate plates were revealed by SEM analysis to remain unchanged.

To evaluate the FE properties of the novel WOP structures, they were tested as field emitters both after preparation and on a new substrate. **Figure 4**a compares the emission current density versus the applied electric field curves (*J*–*E*), recorded at an anode sample distance of 200 μm, for the as-grown and transferred ZnO WOP structures, as well as their conventional ZnO nanowire counterparts (Figure S6, Supporting Information) prepared in a similar CVD process and for the same growth time. It can be seen that the emission current density *J* exponentially increases with the applied field *E* for all three of the samples. Here, the turn-on field ($E_{to}$) and threshold field ($E_{thr}$) can be defined as the electric fields required to produce a current density of 10 μA/cm$^2$ and 1 mA/cm$^2$, respectively. The transferred (and better vertically allined) WOP nanostructures are clearly seen to demonstrate the best FE properties, the lowest turn-on field being 4.8 V/μm, the lowest threshold field being 8.1 V/μm and the highest maximum of emission current density being 7.8 mA/cm$^2$. Meanwhile, the turn-on fields of the as-prepared WOP sample and of conventional CVD-prepared nanowires (also prepared for 60 min) were 5.0 and 6.8 V/μm, respectively (as shown in **Table 1**). The results confirm that the ZnO WOP nanostructures reported in this study are highly transferable field emitters superior to their conventional CVD-grown ZnO nanowire counterparts.

The acquired FE current-voltage characteristics were further analyzed by means of the Fowler–Nordheim (F–N) equation

$$\ln(\mathrm{J})\,\mathrm{E}^2) = \ln(A\beta^2/\phi) - B\phi^{3/2}/\beta E \quad (1)$$

where *A* and *B* are constants with the values of $1.54\times10^{-6}$ A eV V$^{-2}$ and $6.83\times10^3$ V μm$^{-1}$ eV$^{-3/2}$, *J* is the current density, $\beta$ is the field enhancement factor, *E* is the applied field, and $\Phi$ is the work function of the emitting material, which is 5.3 for ZnO. Generally, the value of $\beta$ is related to the emitter geometry, crystal structure and vacuum gaps, and is considered to be an important factor of merit for FE performance. The transferred ZnO WOP structures are seen in Table 1 to demonstrate a very attractive $\beta$ value (1004), which is superior to those of the as-prepared WOP structures (883) and conventional ZnO nanowires (694). The $\beta$ value of the transferred WOP structures is significantly larger than that of the conventional ZnO nanowires and even (surprisingly) than that of the as-prepared WOP structures, being on the level sufficient for various FE applications. We speculate that the better

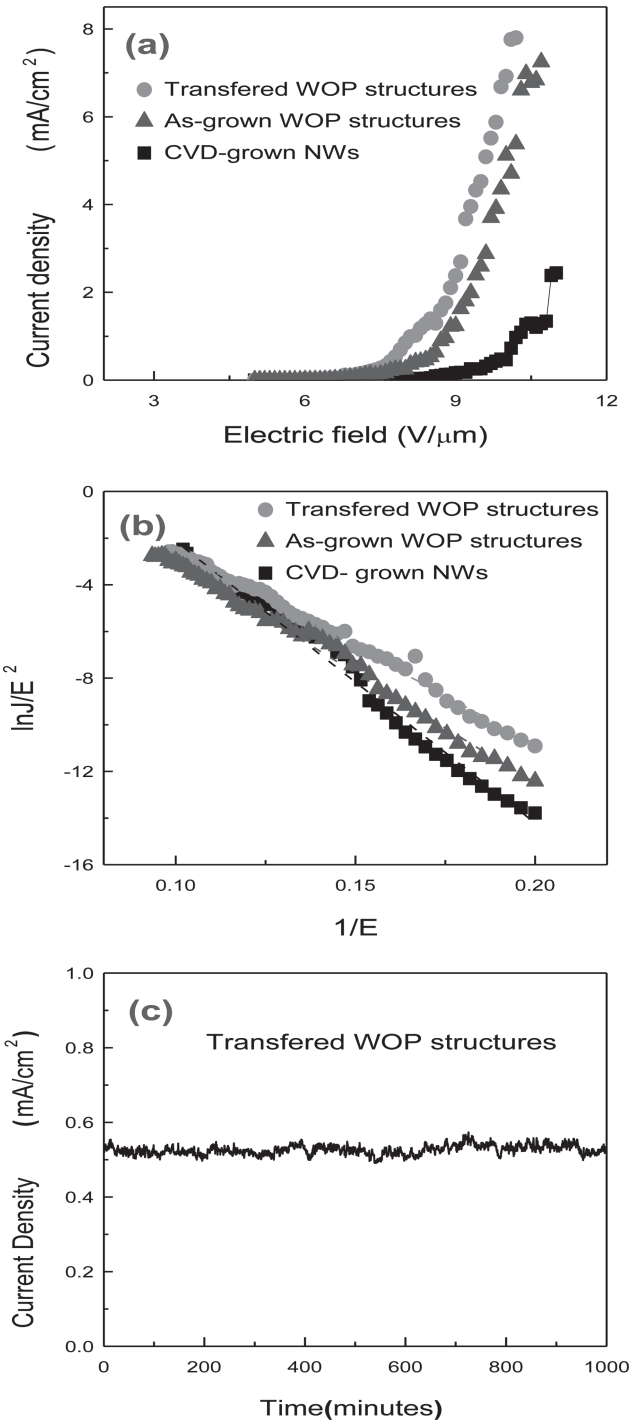


**Figure 4.** *J*–*E* (a) and Fowler–Nordheim (F–N) (b) plots for as-grown and tranferred ZnO WOP structures and for conventional ZnO NWs prepared via CVD grown. c) Field-emission current density of transferred ZnO WOP structures recorded over 1000 min under applied electric field of 8 V/μm.

FE performance of the transferred ZnO WOP structures is explained by their improved vertical orientation, as shown in Figure 2b,c. Thus, the newly prepared nanostructures are 'truly transferable', as their FE performance is enhanced on transferring onto their new host surface. Compared to

**Table 1.** Summary of the main field-emission parameters for as-grown and tranferred ZnO WOP structures and their conventional nanowire counterparts grown via CVD.

| Structure | Turn-on field [V/μm] | Threshold field [V/μm] | $\beta$ |
|---|---|---|---|
| Transferred WOP structures | 4.8 | 8.1 | 1004 |
| As-grown WOP structures | 5.0 | 8.8 | 883 |
| CVD-grown nanowires | 6.8 | 12.2 | 694 |

the conventional CVD-grown nanowires (see Figure S6, Supporting Information), the WOP nanomaterials are nail-like-shaped, which results in the needlepoint effect during electron emission and makes them more efficient emitters than the ZnO nanowires grown under same conditions. Moreover, the FE performance of such ZnO WOP structures is also affected by the length of nanowires, being improved with synthesis time (Figure S7, Supporting Information). This trend, however, was found to change at growth times ≥2 h, when the nanowires were observed to entangle each other. As a result, it become more difficult for them to form vertical arrays, leading to poorer FE performance of the material. The nanostructures grown for 2 h demonstrated the lowest $E_{to}$ value of 6.2 V/μm, the lowest $E_{thr}$ value of 10.3 V/μm, the highest maximum of emission current density of 3.1 mA/cm$^2$, and the $\beta$ value of 796. Thus, the optimal growth time found in the present work was ≈60 min.

Figure 4b presents the F–N plots, $\ln(J/E^2)$ versus $1/E$, for the same samples as in Figure 4a. The F–N plots in Figure 4b are seen to have approximately linear relationships within the measurement range, which confirms that the electron emission from all the ZnO nanostructures follows the F–N behavior. The field enhencement factors obtained from the simulation of the F–N plots in accordace with the above equations are also summerized in Table 1. Stability of the field emitters is another important issue that is closely related to their potential applications. Figure 4c shows the variation of emission current density of transferred ZnO WOP nanostructures measured over a period of ≈1000 min at an applied electric field of 8 V/μm. The emission current density was observed to fluctuate only within 9.4%, proving a high stability of the emitters. The stable FE performance observed for the WOP structures is believed to be related to their sharp nanowire/substrate interface, which results in a very low thermal effect. The good emission stability suggests that such transferable WOP nanostructures can find potential applications in cold-cathode-based electronics.

In summary, we prepared novel ZnO nanostructures grown as single epitaxial wires at the centers of nanoplates via the vapor-phase transport method with a very high selectivity. The sharp interfaces between the wires and nanoplates provide the material with high field-emission properties, while its freestanding nature and the ability to self-align on a new substrate make it extremely attractive as a transferable field emitter. The turn-on field, threshold field, and field enhancement factor of the novel emitters could reach 4.8 V μm$^{-1}$, 8.1 V μm$^{-1}$, and 1004, respectively. These results suggest that the newly prepared ZnO nanostructures are highly promising as materials for transferable and flexible electronic devices.

## Experimental Section

*Epitaxial Growth of ZnO Nanowires on Plates*: ZnO nanoplates were prepared via a simple method previously reported elsewhere.[38,39] Their dispersion in ethanol was prepared by sonication for 5 min. Then the ZnO nanoplates were spin-coated on a heavily doped (100) Si substrate (n-type, resistivity: 6~10 Ω·cm). Prior to spin coating, the substrate was cleaned twice in acetone by sonication for 15 min. A precursor mixture consisting of equal amounts of ZnO (99.99% purity, Aladdin reagent) and graphite (99.95% purity, Aladdin reagent) powders was placed in an alumina boat located at the center of a smaller quartz tube (diameter ≈40 mm). The Si substrate was placed next to the precursor downstream a flowing Ar gas, and the distance between the Si substrate and alumina boat was ≈18 cm. Then they were placed into a larger quartz tube (diameter ≈60 mm) inside a furnace. The boat with precursor was heated to 950 °C. The temperature was reached during 1.5 h and then held for 60 min under 150 mbar at a constant Ar gas flow of 100 sccm. Then the furnace was turned off and cooled to room temperature under an Ar flow. The schematic diagram of the experimental apparatus and its main parameters are given in Figure S8, Supporting Information.

*Transfer of ZnO Nanowires on Plates*: The as-prepared ZnO wire-on-plate sample (on Si substrate) was placed in a 10 mL beaker with 4 mL of ethanol and sonicated for 5 min. The ethanol dispersion with the ZnO wire-on-plate nanostructures was then drop-coated on a new Si or flexible PET/ITO substrate for further measurements.

*Characterization and Field Emission Measurements*: The samples were characterized by field emission scanning electron microscopy (SEM, JEOL JSM-6700F). The field emission properties of different samples (on Si or PET/ITO substrates) were studied at room temperature in a high vacuum chamber ($10^{-6}$ Pa) using a 1 mm$^2$ cross-sectional area aluminum anode. A dc voltage sweeping from 200 to 1100 V was applied to a sample at a step of 50 V. The distance between the electrodes was 200 μm.

## Supporting Information

Supporting Information is available from the Wiley Online Library or from the author.

## Acknowledgements

This work was supported by the National 973 project from the Ministry of Science and Technology, China, the National Natural Science Foundation of China (61222403 and 11274173), the Doctoral Program Foundation from the Ministry of Education of China (20123218110030), the Fundamental Research Funds for the Central Universities (30920130111017 and NE2012004) and the Opened Fund of the State Key Laboratory on Integrated Optoelectronics (IOSKL2012KF06).

Received: May 13, 2013
Revised: June 13, 2013
Published online: July 29, 2013

[1] G. Zhu, R. Yang, S. Wang, Z. L. Wang, *Nano Lett.* **2010**, *10*, 3151.
[2] X. D. Wang, J. Zhou, C. S. Lao, J. H. Song, N. S. Xu, Z. L. Wang, *Adv. Mater.* **2007**, *19*, 1627.
[3] J. She, Z. Xiao, Y. Yang, S. Deng, J. Chen, G. Yang, N. Xu, *ACS Nano* **2008**, *2*, 2015.

[4] K. H. Lee, G. Lee, K. Lee, M. S. Oh, S. Im, S. M. Yoon, *Adv. Mater.* **2009**, *21*, 4287.
[5] A. Nadarajah, R. C. Word, J. Meiss, R. Konenkamp, *Nano Lett.* **2008**, *8*, 534.
[6] Y. He, J. A. Wang, W. F. Zhang, J. Z. Song, C. L. Pei, X. B. Chen, *J. Nanosci. Nanotechnol.* **2010**, *10*, 7254.
[7] H. Zeng, X. Xu, Y. Bando, U. K. Gautam, T. Zhai, X. Fang, B. Liu, D. Golberg, *Adv. Funct. Mater.* **2009**, *19*, 3165.
[8] R. Chen, Q. Ye, T. He, T. Van Duong, Y. Ying, Y. Y. Tay, T. Wu, H. Sun, *Nano Lett.* **2013**, *13*, 734.
[9] S. A. Kulinich, T. Kondo, Y. Shimizu, T. Ito, *J. Appl. Phys.* **2013**, *113*, 033509.
[10] D. Pradhan, M. Kumar, Y. Ando, K. T. Leung, *ACS Appl. Mater. Inter.* **2009**, *1*, 789.
[11] D. Banerjee, S. H. Jo, Z. F. Ren, *Adv. Mater.* **2004**, *16*, 2028.
[12] M. H. Huang, Y. Y. Wu, H. Feick, N. Tran, E. Weber, P. D. Yang, *Adv. Mater.* **2001**, *13*, 113.
[13] S. H. Jo, J. Y. Lao, Z. F. Ren, R. A. Farrer, T. Baldacchini, J. T. Fourkas, *Appl. Phys. Lett.* **2003**, *83*, 4821.
[14] H. Zeng, G. Duan, Y. Li, S. Yang, X. Xu, W. Cai, *Adv. Funct. Mater.* **2010**, *20*, 561.
[15] J. G. Ok, S. H. Tawfick, K. A. Juggernauth, K. Sun, Y. Zhang, A. J. Hart, *Adv. Funct. Mater.* **2010**, *20*, 2470.
[16] J. Yang, M. S. Lee, H. J. Lee, H. Kim, *Appl. Phys. Lett.* **2011**, *98*, 253106.
[17] M. Kevin, W. H. Tho, G. W. Ho, *J. Mater. Chem.* **2012**, *22*, 16442.
[18] K. Wang, J. J. Chen, W. L. Zhou, Y. Zhang, Y. F. Yan, J. Pern, A. Mascarenhas, *Adv. Mater.* **2008**, *20*, 3248.
[19] C. Soci, A. Zhang, B. Xiang, S. A. Dayeh, D. P. R. Aplin, J. Park, X. Y. Bao, Y. H. Lo, D. Wang, *Nano Lett.* **2007**, *7*, 1003.
[20] M. C. Jeong, B. Y. Oh, M. H. Ham, S. W. Lee, J. M. Myoung, *Small* **2007**, *3*, 568.
[21] B. Q. Cao, W. P. Cai, G. T. Duan, Y. Li, Q. Zhao, D. P. Yu, *Nanotechnology* **2005**, *16*, 2567.
[22] L. Schmidt-Mende, J. L. MacManus-Driscoll, *Mater Today* **2007**, *10*, 40.
[23] P. X. Gao, Y. Ding, I. L. Wang, *Nano Lett.* **2003**, *3*, 1315.
[24] G. Perillat-Merceroz, R. Thierry, P. H. Jouneau, P. Ferret, G. Feuillet, *Nanotechnology* **2012**, *23*, 125702.
[25] X. Huang, L. Shao, G. W. She, M. Wang, S. Chen, X. M. Meng, *Crystengcomm* **2012**, *14*, 8330.
[26] S. H. Yi, S. K. Choi, J. M. Jang, J. A. Kim, W. G. Jung, *J. Colloid. Interf. Sci.* **2007**, *313*, 705.
[27] T. Pauporté, G. Bataille, L. Joulaud, F. J. Vermersch, *J. Phys. Chem. C* **2009**, *114*, 194.
[28] S. Y. Li, C. Y. Lee, T. Y. Tseng, *J. Cryst. Growth* **2003**, *247*, 357.
[29] G. Kresse, O. Dulub, U. Diebold, *Phys. Rev. B* **2003**, *68*, 245409.
[30] P. X. Gao, Z. L. Wang, *J. Phys. Chem. B* **2002**, *106*, 12653.
[31] S. Cho, J. W. Jang, J. S. Lee, K. H. Lee, *Nanoscale* **2010**, *2*, 2199.
[32] C. Cheng, B. Liu, H. Yang, W. Zhou, L. Sun, R. Chen, S. F. Yu, J. Zhang, H. Gong, H. Sun, H. J. Fan, *ACS Nano* **2009**, *3*, 3069.
[33] N. N. Fan, Y. Yang, W. F. Wang, L. J. Zhang, W. Chen, C. Zou, S. M. Huang, *ACS Nano* **2012**, *6*, 4072.
[34] A. R. Tao, S. Habas, P. Yang, *Small* **2008**, *4*, 310.
[35] A. Wei, X. W. Sun, C. X. Xu, Z. L. Dong, Y. Yang, S. T. Tan, W. Huang, *Nanotechnology* **2006**, *17*, 1740.
[36] J. H. Song, F. Kim, D. Kim, P. Yang, *Chem. Eur. J* **2005**, *11*, 910.
[37] F. Li, Y. Ding, P. Gao, X. Xin, Z. L. Wang, *Angew. Chem. Int. Edit.* **2004**, *43*, 5238.
[38] B. Q. Cao, W. P. Cai, Y. Li, F. Q. Sun, L. D. Zhang, *Nanotechnology* **2005**, *16*, 1734.
[39] X. Cao, H. Zeng, M. Wang, X. Xu, M. Fang, S. Ji, L. Zhang, *J. Phys. Chem. C* **2008**, *112*, 5267.